International Journal of Thermophysics, Vol. 27, No. 1, January 2006 (© 2006)
DOI: 10.1007/s10765-006-0042-5

Thermophysical Analysis of Sandstone by Pulse Transient Method[1]

Ľ. Kubičár,[2,3] V. Vretenár,[2] V. Boháč,[2] and P. Tiano[4]

Stones belong to porous materials where water in pores plays an important role during the freeze–thaw process. A thermophysical analysis based on the pulse transient method has been used to study an ageing cycle, namely the freeze–thaw cycle. Thermophysical analysis is based on measuring the thermophysical properties under specific thermodynamic conditions. The transient method determines the specific heat, thermal diffusivity, and thermal conductivity by a single measurement. A specimen of Sander sandstone was analyzed in both dry and water-saturated states. Typical anomalies of all thermophysical parameters at the freeze–thaw point as well as differences for the dry and saturated states were found. The changes of thermophysical parameters measured when using freeze–thaw cycles correspond to stone ageing. The freeze–thaw cycle can often be encountered in building physics, concrete construction, etc.

KEY WORDS: ageing process; freeze–thaw cycle; moisture content; pulse transient method; sandstone; specific heat; thermal conductivity; thermal diffusivity.

1. INTRODUCTION

Freeze–thaw processes in a porous structure significantly influence durability and application of stones in practice. The pore structure strongly affects local stress resulting from the volume change of a fluid under freezing conditions and can lead to its fracturing. Thus, the pore shape, volume

[1] Paper presented at the Seventh Asian Thermophysical Properties Conference, August 23–28, 2004, Hefei and Huangshan, Anhui, P. R. China.
[2] Institute of Physics, SAS, Dúbravská cesta 9, 845 11 Bratislava, Slovakia.
[3] To whom correspondence should be addressed. E-mail: kubicar@savba.sk
[4] CNR – ICVBC – Via Madonna del Piano, Edificio C, 50019 Sesto Fiorentino, Italy.

distribution, and permeability are relevant to the reliability of a rock in an environmental application, e.g., in building physics. Extensive experimental and theoretical research has been carried out to find methods for studying rock durability in civil engineering application, hydro-geological studies, utilization of hydro-thermal energy, underground storage, etc. considering the internal structure of pore space and the corresponding transport of fluid through the pores and heat through the rock skeleton.

Many different properties of materials are used to study rock degradation under weathering cycles: sound velocity [1–3], thermal conductivity [4], permeability [5–7], saturation [8], shape [5] and size distribution of pores [8], internal surface [5], and grain bonds [5].

A number of experimental methods have been developed to investigate heat transport through material structures. Generally, they can be divided into two groups, namely steady-state [9] and transient [10] methods. The first of the two groups needs long measuring times, and allows redistribution of the fluid in the porous structure; thus, the information obtained is far away from the thermodynamic state needed. Transient methods require significantly shorter measuring times, so the information obtained corresponds to the thermodynamic state found in real applications.

In this paper, we present results of a thermophysical analysis based on measurements of specific heat, thermal diffusivity, and thermal conductivity by the pulse transient method. Sander sandstone was used for the thermophysical analysis. The freeze–thaw cycle representing the artificial ageing (AA) process is analyzed for dry and water-saturated Sander sandstone. The corresponding skeleton damage of the stone is analyzed using heat-transport parameters, thermal conductivity and thermal diffusivity, and the specific heat as a calorimetric parameter that can be calculated from the volumetric specific heat using density [12].

2. EXPERIMENTAL METHOD

A pulse transient method is used for measuring thermophysical parameters [11]. The principle of the method is shown in Fig. 1. The specimen consists of three parts (I, II, III). A resistive plane heat source is clamped between the first and second parts. One junction of a thermocouple is placed between the second and third parts, where it measures the temperature response to the heat pulse. The ideal model of the pulse transient method yields the relation,

$$T(h,t) = \frac{Q}{c_p \rho \sqrt{\pi a t}} \exp\left(-\frac{h^2}{4at}\right), \tag{1}$$

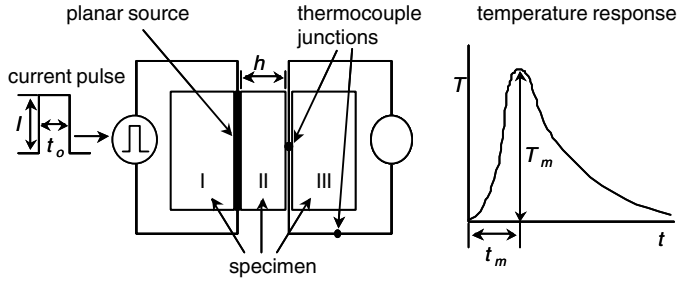

Fig. 1. Principle of the pulse transient method.

for the transient temperature $T(h,t)$ at the thermocouple junction. Here, $Q = RI^2t_0$ represents the energy of the heat pulse released per unit area, R is the electrical resistance of the unit area of the heat source, t_0 is the width of the heat pulse, t is the time, and h is the distance between the heat source and the thermocouple junction. For the sample, ρ is the density, c_p is the specific heat, and a is the thermal diffusivity (Fig. 1). Equation (1) is valid for a non-limited body in which an ideal heat source produces a heat pulse in the form of a Dirac delta pulse. In a real situation the specimen is limited and a real width of the heat pulse t_0 is used.

The standard one-point evaluation procedure considers the maximum of the temperature response T_m for the calculation of the thermophysical parameters, as follows [11]; specific heat:

$$c_p = Qf_\mathrm{c}/\sqrt{2\pi e}\rho h T_\mathrm{m} \tag{2}$$

thermal diffusivity:

$$a = h^2/2t_\mathrm{m} f_\mathrm{a} \tag{3}$$

and thermal conductivity

$$\lambda = ac_p\rho = Qhf_\mathrm{c}/2\sqrt{2\pi e}t_\mathrm{m}T_\mathrm{m}f_\mathrm{a} \tag{4}$$

where $Q = RI^2t_0$ ($R[\Omega\cdot\mathrm{m}^{-2}]$ is the resistance of the planar heat source, I [A] is the electrical current—see Fig. 1, t_0 [s] is the width of the heat pulse, T_m represents the maximum temperature response at the time t_m, e denotes the Euler number, and f_a, f_c are correction factors [11]. The correction factors f_a and f_c characterize deviations from the ideal model.

3. SPECIMEN

The specimen setup consists of three blocks, each with a cross section of $50 \times 50\,\text{mm}^2$, and thicknesses, $h_1 = 50\,\text{mm}$, $h_2 = 12\,\text{mm}$, and $h_3 = 38\,\text{mm}$. The size of the blocks was chosen considering suppression of the heat losses from the specimen surface in the radial direction. The infinite media was created in the axial direction by contact of the outer blocks with the heat exchangers. Thus, the specimen size represents a criterion of the ideal model. The specimen was cut from sandstone from Sander Schilfsandsteinbruch "Hermannsberg", Hassberge, Germany. Basic characteristics of the specimen are given in Table I.

The dry state was reached within a drying cycle at 60°C for 2 h, followed by reweighing at 25°C. The cycling was repeated until the limit in mass change between two consecutive cycles was less then 0.1%. The water-saturated state was reached by immersing the specimen into distilled water for 2 h followed by reweighing. This cycling was repeated until the mass change between two consecutive weighings was less than 0.3%.

The ageing procedure consists of freeze–thaw cycles of the water-saturated specimen. A freezing box at −18°C and a temperature box at 25°C were used for the freeze–thaw cycle. The water-saturated specimen was alternatively placed into the freezing box and the room temperature box, each for 2 h, to induce an artificial ageing (AA) cycle. Typically, 10AA cycles were performed. Then a drying procedure was realized, followed by measuring of the thermophysical properties. The moisturizing procedure was, again, followed by 10 AA cycles. The specimen drying and the measuring of thermophysical parameters were repeated several times. Finally, 60 AA cycles were performed to establish variations in measured parameters due to stone degradation. No visible damage was found after 60 AA cycles.

4. MEASURING PROCEDURE

The instrument, RTB 1.01 (Transient MS), is used for measuring the thermophysical properties. The basic scheme of the instrument is shown in Fig. 2. The thermostat in connection with the plate heat exchangers

Table I. Basic Characteristics of the Sander Sandstone Specimen

Bulk density ($\text{kg} \cdot \text{m}^{-3}$)		Water porosity (%)	
Dry	Water-saturated	Calculated	Published [16]
2175	2315	14	17.8

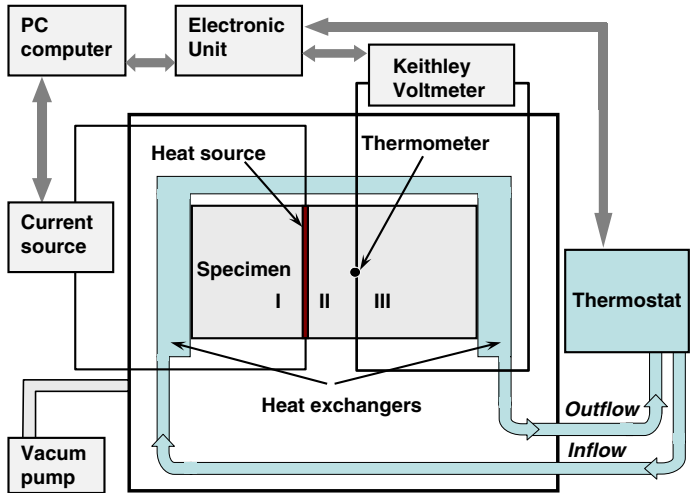

Fig. 2. Schematic of the instrument RT 1.02 for thermophysical analysis.

establishes the specimen temperature. Both a non-isothermal measuring regime with heating and cooling rates of $0.01\,\mathrm{K}\cdot\mathrm{min}^{-1}$ and an isothermal one with an isotherm within the limit of 0.02 K were used. The non-isothermal regime was used to study freezing and thawing phenomena. A negligible temperature gradient across the specimen was assumed to be established using the non-isothermal measuring regime with heating and cooling rates of $0.01\,\mathrm{K}\cdot\mathrm{min}^{-1}$. The isothermal measuring regime was used to measure the thermophysical parameters and to study the AA cycles.

A programmable current source (Kepco) was used for generation of the heat pulse using a planar resistance of 2 Ω. The planar heat source was made of a 20 μm thick nickel foil that was etched in the form of a meander and covered between with 25 μm thick Kapton foil (Transient MS). Heat pulses having a width period of 5.5–8 s and energy in the range from 60 to $125\,\mathrm{kJ}\cdot\mathrm{m}^{-2}$ were used. The temperature response was scanned by a Keithley voltmeter. A pc controls all units. An automatic evaluation procedure was used in connection with the RTB 1.01 instrument using Eqs. (2)–(4) where correction factors f_a and f_c considering the non-ideal width of the heat pulse were calculated according to the procedure described elsewhere [11].

An uncertainty analysis was performed considering a one-point evaluation procedure for a specimen thickness of $h = 12.4\,\mathrm{mm}$, a heat pulse energy of $Q = 79\,\mathrm{kJ}\cdot\mathrm{m}^{-2}$, a temperature response $T_m \sim 1\,\mathrm{K}$, and $t_m = 76.8\,\mathrm{s}$. Data reduction expression (Eqs. (2)–(4)) include uncertainties of the heat pulse energy $Q = U_h \frac{U_I}{R_s} t_0$, where $U_h = 8.25\,\mathrm{V}$ is the voltage measured

across the heater resistance and the current standard resistance $R_s = 0.4\,\Omega$ is measured with a voltage $U_I = 1.75\,V$. Both voltages, each having 100 scans, are scanned by using a 16 bit A/D converter. The corresponding standard deviations u_{U_h} and u_{U_I} are 0.01 and 0.05%, respectively, and the uncertainty in resistance is $u_{R_s} = 0.004\,\Omega$. The heat pulse energy is recalculated for a unit of the specimen cross section F with a precision of 1.4%. The supplier/producer of the K-type thermocouple (Omega) specifies its uncertainty to be better than 0.75% of the measured value at 25°C and a temperature response of $T_m \sim 1\,K$, while the use of the Keithley voltmeter introduces 0.03% uncertainty and measuring the maximum temperature response T_m induces an additional uncertainty of 1.25%.

The uncertainty budget has been compiled assuming the validity of a model which includes the real heat pulse width [12]. Table II gives an overview of individual components of the overall uncertainty.

The values of the overall uncertainties estimated for the one-point evaluation procedure are 5.88% for the thermal diffusivity, 3.97% for the specific heat, and 3.91% for the thermal conductivity.

5. EXPERIMENTAL DATA AND DISCUSSION

Data on the thermophysical parameters of dry and water-saturated sandstone are shown in Fig. 3. Anomalies of the thermophysical parameters were found for the water-saturated state while no anomalies exist for dry stones. A hysteresis was found for all the thermophysical parameters of the water-saturated structure, considering the heating and cooling measuring regimes.

Table III shows the variations of the thermophysical properties of the dry and water-saturated sandstones at 1.5°C, when the water in the pores was in a fluid state, and at −10°C when water in the pores was frozen.

Table II. Uncertainty Budget for Specimen Thickness $h = 12.4\,mm$ at 25°C

Parameter	Value	Estimated uncertainty	Uncertainty type	Uncertainty contribution
h(m)	0.0124	0.00035	B	2.85%
Q (kJ·m^{-2})	79.37	1.37	Combined	1.73%
ρ(kg·m^{-3})	2175	34	B	1.58%
T_m(°C)	0.839	0.012	B	1.46%
t_m (s)	76.8	1.1	B	1.43%
f_a	0.9633	0.0006	B	0.06%
f_c	1.001	0.0001	B	0.01%

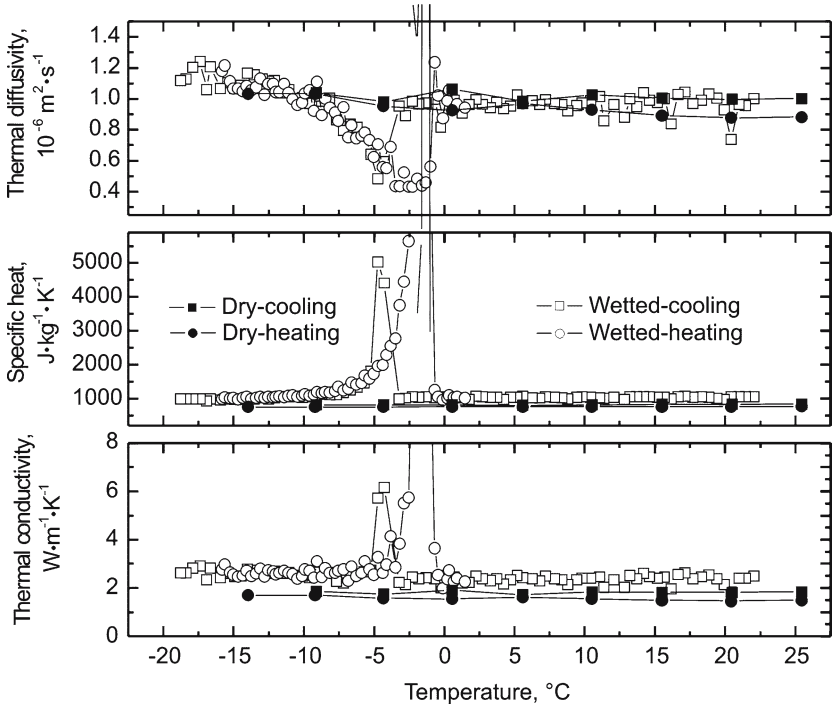

Fig. 3. Thermophysical properties of Sander sandstone for dry and water-saturated states during cooling and heating in a temperature range from –20 to 25°C.

Table III. Thermophysical Properties of Sander Sandstone for Dry and Water-Saturated State

Parameter	Dried		Water-saturated	
	1.5°C	–10°C	1.5 °C	–10°C
Thermal diffusivity (10^{-6} m^{-2} s^{-1})	1.04	1.03	0.99	1.10
	–1.0%		+11.1%	
	–4.8%			
Specific heat (J kg^{-1} K^{-1})	814	799	1045	992
	–1.8%		–5.1%	
	28%			
Thermal conductivity (W m^{-1} K^{-1})	1.89	1.85	2.45	2.6
	–2.1%		+6.1%	
	29%			

While the difference in the thermal diffusivity for the dry and the water-saturated states is less than 5%, a significantly larger difference exists in the specific heat value, i.e., more than 24% for both temperatures ($-10°C$ and $1.5°C$).

Thermophysical data on air, water, and ice are given in Table IV. Different experimental conditions caused a rather wide range of variations of thermophysical parameters of pore contents during the experiment. The thermal diffusivity is a function of the sound velocity and mean free path of phonons [13]. A small variation of the thermal diffusivity with the pore content does not indicate that the pores play a predominant role in heat transport. However, the specific heat indicates that the pore content influences the thermodynamics of the sandstone under test. This is a consequence of the significant differences in the heat capacities (Volumetric specific heats) of air, water, and ice (see Table IV).

Deviations in specific heat from equilibrium values for inhomogeneous materials might occur when dynamic measuring methods are used [14]. Therefore, a test of the mixing rule was performed when the pores were filled with air, water, and ice. It is assumed that the experimental value of the volumetric specific heat for the dry state corresponds to the sandstone because of the negligible contribution of pores filled by air (see Table IV). The experimental and calculated data of the volumetric specific heat (heat capacity) are shown in Table V. A negligible difference exists between the calculated and measured volumetric specific heats for wet sandstone while there occurs a difference of 14%, which is significantly larger than the measuring error, when pores are filled by ice. A mixing rule for the latter case is not satisfied. Thus, one obtains an apparent value of the specific heat. Clearly, the thermal diffusivity controls the validity of the mixing rule when transient methods are used for measuring thermophysical properties.

Several authors discuss the role of water in pores by modeling [2, 3] and analyzing thermal conductivity data [4]. The mentioned thermophysical

Table IV. Thermophysical Property Data of Air, Water, and Ice

Parameter	Air – dry	Water	Ice
Thermal diffusivity (10^{-6} $m^2 \cdot s^{-1}$)	27	0.14	1.1
Specific heat ($J \cdot kg^{-1} \cdot K^{-1}$)	716	4226	2135
Thermal conductivity ($W \cdot m^{-1} \cdot K^{-1}$)	27	0.14	1.1
Density ($kg \cdot m^{-3}$)	1.29	1000	920
Volumetric specific heat ($kJ \cdot m^{-3} \cdot K^{-1}$)	0.923	4226	1964

Table V. Test of the Mixing Rule for the Volumetric Specific Heat of Sandstone

Sandstone		Volumetric specific heat ($MJ \cdot m^{-3} \cdot K^{-1}$)	
		+1.5°C (Water)	−10°C (Ice)
Dry	Measured	1.77	1.74
Wet	Measured	2.42	2.30
	Calculated	2.36	2.04

parameters are inter-related by the relation $\lambda = ac\rho$. Thus, our data indicate that thermal conductivity variations are caused by the heat capacity changes, dependent on the pore contents. Therefore, detailed information on pore structure and its contents must be known to understand the results of the specific heat and thermal conductivity.

Specific heat anomalies during cooling (up) and heating (down) are shown in Fig. 4 as a function of temperature. Different heat pulse energies were used. While a complicated structure of the specific heat curves was found for a cooling cycle (two peaks anomaly), a one-peak anomaly was measured during heating. The solidification (freezing) phenomenon is a complicated function of the droplet size—pore volume and its interaction with the pore surface [15]. Thermodynamics of the pore content determines formation of the nucleus and the solid phase growth.

The pores of the sandstone have a broad distribution with two peaks, namely, in the vicinity of 0.064 and 4 μm [16]. The size distribution of the pores vs. the total effective porosity is shown in Fig. 5. The effective porosity includes open pores only [17]. Thus, the diameter of throats and the size of pores are critical parameters for the degree of the water saturation of sandstone. Therefore, there are different conditions for formation of nuclei for small and for large pores—droplet sizes [15]. Thus, two peaks of the size distribution of the pores could correspond to those found in specific heat at freezing. On the contrary, the thawing phenomenon indicates a one-peak anomaly in accordance with the specification of the reference point, 0°C, of the temperature scale even though there is a small deviation found for the highest heat pulse.

The latent heat for the freezing and thawing processes was determined, and the results are shown in Fig. 6, both for cooling (up) and for heating (down). The latent heat was determined by integration of an area below the specific heat peaks. A significantly smaller latent heat was found in the cooling regime. The recalculated latent heat for 14% porosity gives a value of $324\,kJ \cdot kg^{-1}$, which is close to the tabulated value of $333\,kJ \cdot kg^{-1}$

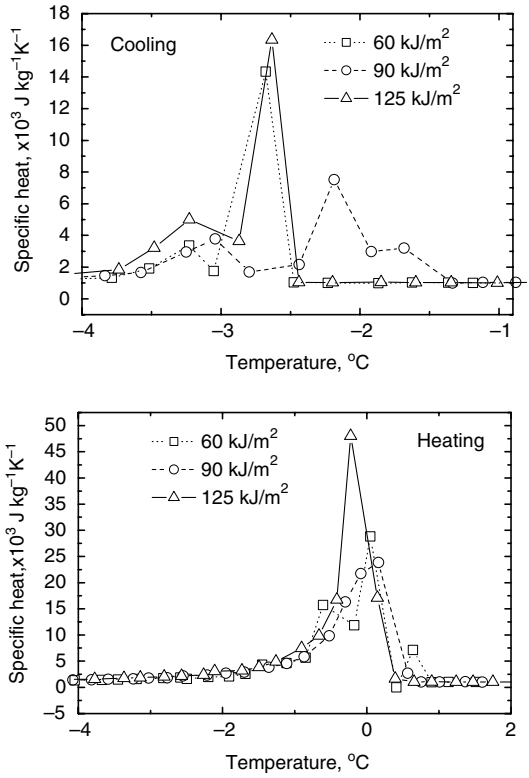

Fig. 4. Specific heat anomalies of Sander sandstone during cooling and heating. Parameter: heat pulse energy.

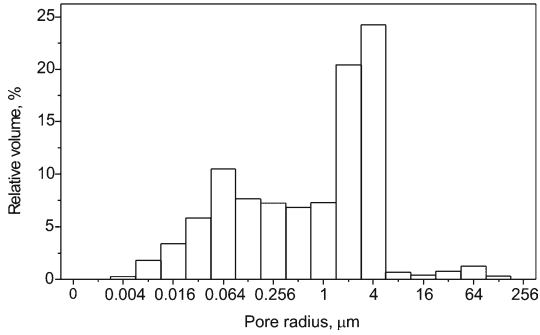

Fig. 5. Distribution of pore sizes in sandstone.

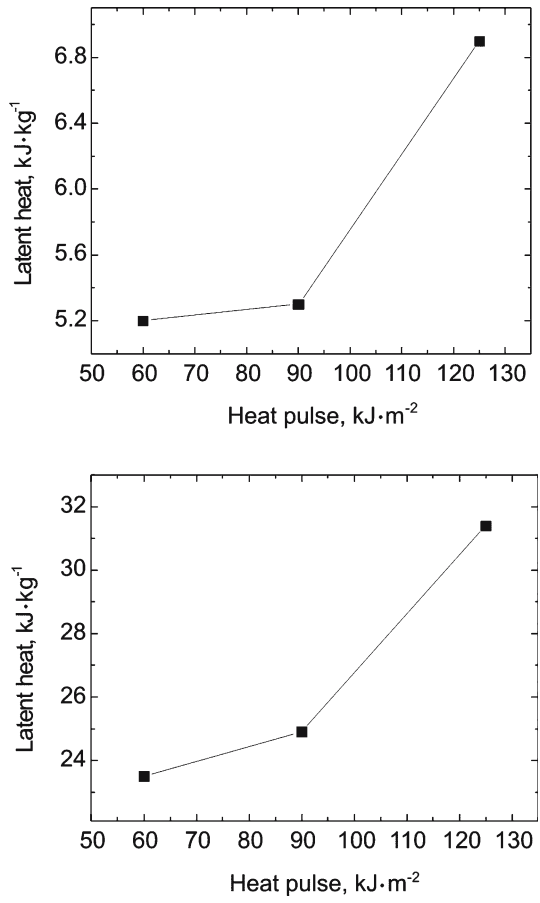

Fig. 6. Latent heat of freezing (up) and thawing (down) of water-saturated Sander sandstone calculated from specific heat anomalies.

for the heating regime. A strong non-linearity was found for heat pulse energies above $100\,\mathrm{kJ}\cdot\mathrm{m}^{-2}$. Anomalies of the specific heat and the thermal diffusivity have a clear physical foundation. While the former is connected with the latent heat ascribed to the phase change, the latter one is accompanied with the strong ultrasound attenuation and a decrease of the acoustic velocities [18]. However, the thermal conductivity has an apparent anomaly originating from the consistency relation, $\lambda = ac\rho$. In fact, the thermal conductivity is experimentally not detectable in a material volume, where a phase transition of the first order is occurring, because the

temperature gradient vanishes. Therefore, well defined clear values of the thermal conductivity can be established only below and above the phase transition. Kinetic processes are occurring within phase transitions that are characterized by different parameters such as the activation energy, growth, etc.

The model of the measuring method is based on a homogenous medium where the measuring process does not generate any non-linearities considering transients of the temperature. However, in this work, we encounter heterogeneous materials composed of two components, namely, the sand and the pore content. The properties of the pore content vary over a wide range of thermophysical parameters. The test of the mixing rule has shown deviations for the specific heat when pores are filled with ice. The apparent specific heat can be determined for this case only. In addition, the model of the pulse transient method assumes equilibrium of the system under test—sandstone—and a small disturbance is applied to it in the form of a heat pulse in order to produce a temperature response. The energy of the heat pulse should be in a range where the evolution of any non-linearity is suppressed. For that case the thermophysical parameters are not a function of the heat pulse energy [18]. The experiments have proved this to be true for the case where the temperature of the specimen is far from the critical one, i.e., from the freezing and thawing point. Figure 6 indicates a strategy for the choice of the heat pulse energy to avoid a possible non-linearity. The heat pulse energy should be well below $90\,\mathrm{kJ}\cdot\mathrm{m}^{-2}$. However, large data scatter was found when using a heat pulse energy that was too small. The working range of the heat pulse energy is from 60 to $90\,\mathrm{kJ}\cdot\mathrm{m}^{-2}$. Nevertheless, a special measuring procedure has to be developed to analyze thermophysical properties around critical points in detail for any material that undergo a phase transition.

Combined heat and mass transfer can occur in porous structures when temperature or mass gradients are established throughout a material under test. However, there is a significant difference between the classic, steady-state methods for measuring thermal conductivity and the pulse transient method. The latter works for equilibrium conditions, i.e., no temperature and mass gradients exist throughout the specimen. The measuring process is completed within 60 s while a small disturbance—a heat pulse—is applied within a limit where no evolution of the mass transport is generated.

The volume change during freezing of water induces damage to the stone. It is believed that the pore distribution is changed and heat–conducting paths are interrupted [1, 19]. Therefore, some AA experiments were performed in which water-saturated Sander sandstone underwent a freeze–thaw process within the temperature range from -18 to $25^{\circ}\mathrm{C}$. The

results are shown in Fig. 7. As we have stressed above, the thermal diffusivity is a heat-transport parameter connected with the elastic properties of the stone skeleton while the specific heat is a thermodynamic parameter. According to the data, the thermal diffusivity has been changed by up to 4%, whereas, the data on the specific heat show scatter. A decrease in the thermal diffusivity indicates degradation of the material. The changes in the thermal diffusivity continue through 10 freeze–thaw cycles.

The thermal diffusivity change shown in Fig. 7 is within its overall uncertainty, i.e., within 5.88%. The greatest contribution to the thermal diffusivity uncertainty is from the specimen thickness uncertainty (see Table II). The bars on the thermal diffusivity data in Fig. 7 represent the reproducibility of the measurements including reassembly. The data show that both components have a lower value than the estimated overall uncertainty. Thus, the mass of the specimen thickness uncertainty is preserved due to the reassembly. The specific heat change in Fig. 7 is within the overall uncertainty of the specific heat, i.e., within 3.97%.

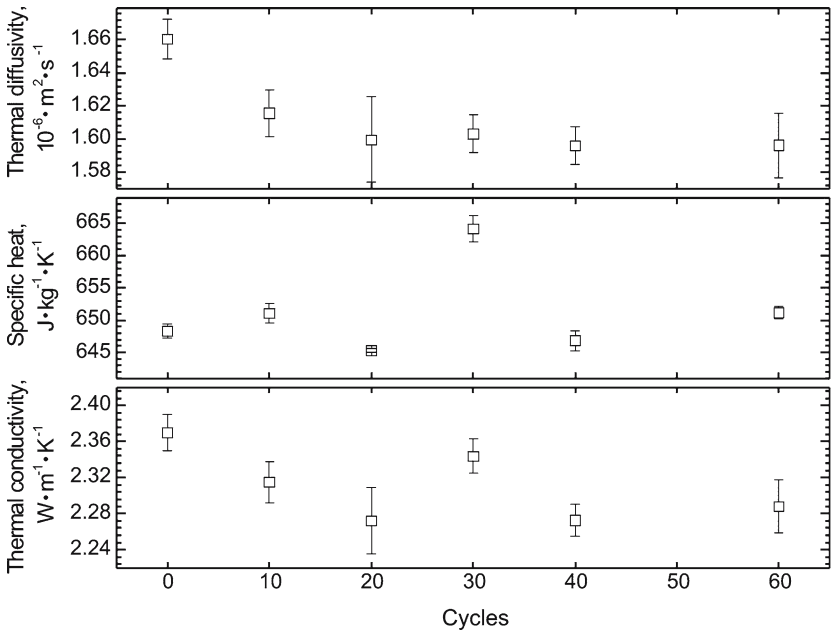

Fig. 7. Change of the thermophysical properties of Sander sandstone due to freeze–thaw cycling.

6. CONCLUSIONS

Thermophysical analysis of Sander sandstone was performed using the pulse transient method for measuring the thermal diffusivity, specific heat, and thermal conductivity. The analysis includes measurements of the thermophysical properties of dry and water-saturated sandstone within the temperature range from -18 to 25°C. Anomalies of the thermophysical properties were investigated during the freeze and thaw processes of water saturated sandstone. An artificial ageing process was studied using several freeze–thaw cycles of water-saturated sandstone followed by measurements of the thermophysical parameters in the dry stage before and after cycling.

Differences in specific heat and thermal conductivity up to 20% and thermal diffusivity of about 5% were found at 1.5 and 18°C, in comparing the dry and water-saturated states. Hysteresis in anomalies of the thermophysical parameters was established within 2.7°C. A two-peak anomaly of the specific heat was found during cooling, whereas a single-peak anomaly exists on heating. The corresponding latent heat by cooling was determined to be 6 $kJ \cdot kg^{-1}$, whereas by heating, 25 $kJ \cdot kg^{-1}$. A decrease of the thermal diffusivity of about 4% within 10 AA cycles while a scatter of the specific heat data of about 2% within 60 AA cycles were found.

The presented results can strongly impact building physics. The following points should be considered in engineering applications, especially for energy transfer calculations in buildings: differences in thermophysical parameters for moist and dry states of the porous materials (bricks, concretes, stones, etc.), existence of latent heat during temperature drop below 0°C and hysteresis of the freezing–thawing point, and material degradation due to freeze/thaw cycles. Pore sizes limit application of the method presented for thermophysical analysis. The governing parameter is specimen size which is limited by dimensions $150 \times 150 \times 200\,mm^3$ for the RTB 1.01 instrument employed here. Then the pore sizes are limited to be no larger than 4–5 mm to obtain representative values of the thermophysical parameters.

ACKNOWLEDGMENTS

This research was carried out under the EU project "MCDUR: Effects of the Weathering on Stone Materials: Assessment of their Mechanical Durability" under Contract G6RD-CT2000-00266. The experimental technique was partly financially supported by project VEGA under Contract No: 2/2036/22. The authors thank the MCDUR partners for support in the development of the proposed methodology. The authors are thankful for permission to use data in Fig. 5, measured by M. Montoto.

REFERENCES

1. T. Popp and H. Kern, *Phys. Chem. Earth* **23**:373 (1998).
2. B. Gurevich and J. M. Carcione, *Pure Appl. Geophys*. **157**:811 (2000).
3. R. J. S. Brown and J. Korringa, *Geophysics* **40**:608 (1975).
4. B. Troschke and H. Burkhardt, *Phys. Chem. Earth* **23**:351 (1998).
5. H. Pape, C. Clauser, and J. Iffland, *Pure Appl. Geophys*. **157**:603 (2000).
6. B. Kieffer, C. F. Jové, E. H. Oelkers, and J. Schott, *Geochimica et Cosmochimica Acta* **63**:3525 (1999).
7. E. Spangenberg, U. Spangenberg, and C. Heindorf, *Phys. Chem. Earth* **23**:367 (1998).
8. D. B. Stephens, K. C. Hsu, M. D. Ankeny, N. Blandford, T. L. Roth, J. A. Kelsey, and J. R. Witworth, *Hydrogeology J*. **6**:156 (1998).
9. K. D. Maglić, A. Cezairliyan, and V. E. Peletsky, eds., in *Compendium of Thermophysical Property Measurement Methods*, Vol. 2, *Recommended Measurement Techniques and Practices* (Plenum Press, New York and London, 1992), p. 643.
10. Ľ. Kubičár and V. Boháč, in *Proc. 24th Int. Thermal Cond./12th Int. Thermal Expansion Symp*., P. S. Gaal and D. E. Apostolescu eds., (Technomic Pub. Co., Pittsburgh, Pennsylvania, 1999), pp. 135–149.
11. Ľ. Kubičár, in *Comprehensive Analytical Chemistry*, G. Svehla ed. (Elsevier, Amsterdam, Tokyo, Oxford, New York, 1990), p. 360
12. *Guide to The Expression of Uncertainty in Measurement*, International Organization for Standardization, ISBN 92-67-10188-9 (ISO, Geneva, 1995).
13. G. Grimvall, in *Selected Topics in Solid State Physics*, Vol. XVIII, E. P. Wohlfarth ed. (North-Holland, Amsterdam, 1968), p. 345
14. Ľ. Kubičár, V. Boháč, V. Vretenár, Š. Barta, G. Neuer, and R. Brandt, *Int. J. Thermophys*. **26**:1949 (2005).
15. H. K. Christenson, *J. Phys.: Condens. Matter* **13**:R95 (2001).
16. M. Montoto, private communication, Dept. of Geology, Group of Petrophysics, University of Oviedo, Oviedo, Spain.
17. M. Montoto, *Petrophysics at the Rock Matrix Scale: Hydraulic Properties and Petrographic Interpretation*, Publication Tecnica 11/2003 (enresa, Direction de Communication C. Emilio Vargas, 7, 28043 Madrid, December 2003), p. 71.
18. Ľ. Kubičár, V. Vretenár, and U. Hammerschmidt, *Int. J. Thermophys*. **26**:507 (2005).
19. V. G. Ruis de Argandona, A. R. Rey, C. Celorio, L. M. Suarez del Rio, L. Caleja, and J. Llavona, *Phys. Chem. Earth (A)* **24**:633 (1999).